INTERNATIONAL BUILDING PERFORMANCE SIMULATION ASSOCIATION ENGLAND

Proceedings of BSO-VI 2022
Sixth Building Simulation and Optimisation Virtual Conference
13 - 14 December 2022
Hosted by University of Bath, UK

Performance evaluation of Phase Change Materials for cooling Photovoltaics and enhancing efficiency in the Global South

(leave this line blank)
A[1], B[2], C[2]
[1]Institution 1, City 1, Country 1
[2]Institution 2, City 2, Country 2
(The names and affiliations SHOULD NOT be included in the draft submitted for review)
(leave blank up to line 10 – remove line numbering from final version)

Abstract

Despite the carbon reduction potential of Photovoltaics (PV) for buildings energy use, its adoption in the residential sector is limited. For effective building integration, it is crucial that PV panels operate close to the standard conditions (~25°C). Overheating of PV in hot climates leads to low PV efficiencies, which can adversely affect the technology adoption. In this study, the effectiveness of Phase Change Materials (PCM) in reducing panel surface temperatures of Concentrated Photovoltaic (CPV) in the Global South (GS) is explored. Utilising lab-based experimental data from a CPV-PCM system, and a co-simulation approach using the software BCVTB, MATLAB (v2018b) and EnergyPlus (v8.8), the panel surface temperature and CPV efficiency were simulated. A total of 128 locations across 17 countries in the GS were identified for simulation that satisfied the following conditions: (i) EnergyPlus weather files (.epw) availability, (ii) yearly averaged diurnal swing greater than 10°C, and (iii) peak summer temperature in excess of 25°C. From the results, we identified 36 locations in the GS where PCM integrated PV resulted in a 2% - 7% relatively improved annual average efficiency over the non-PCM baseline, while in the remaining 92 locations PCMs either did not make a notable improvement or reduced the efficiency.

Key Innovations

- 885 Global South locations were analysed, out of which 128 locations had at least a 10°C monthly average diurnal swing, and sufficiently hot summers to warrant PCM-PV integration.
- PCM-CPV performance was simulated for the selected 128 Global South locations. A co-simulation approach using EnergyPlus was used to facilitate implementation of buildings energy modelling.
- PCM integration resulted in improved performance in 36 locations, because of lower maximum and minimum daily efficiencies – thus preventing poor performance in hot climatic locations.
- PCM integration resulted in a lower average annual efficiency for the remaining majority locations.

Practical Implications

Besides identification of the locations and weather conditions where integrating PCM into PV may prove beneficial, the automated co-simulation approach presented in this study can be utilised to study other novel PV systems for which experimental data may be available but EnergyPlus does not have the capability to model. While 256 co-simulations with different IDFs (EnergyPlus Input Data Files), weather files and experimental data were launched programmatically, a delay of less than 60s between successive simulations resulted in failed BCVTB runs. Thus, the method used in this study is time intensive.

Introduction

Integration of Photovoltaics (PVs) into buildings can contribute to large reductions in carbon emissions, but with a total installed capacity of ~133 GW worldwide (2020 IEA), and a potential of 707.5 GW, solar PV adoption in the residential sector currently only stands at 18%. It is a matter of great concern as countries across the globe work together to contribute to the United Nation Sustainable Development Goals 7 (Affordable and Clean Energy), Goal 9 (Industry, Innovation, and Infrastructure), and Goal 13 (Climate Action).

For effective building integration, it is crucial that the PV panels operate close to the standard temperature conditions (~25°C), Overheating in hot climates leads to reduction in efficiency and panel degradation, leading to shortened lifetime of the PV/CPV panels and impeding its uptake.

In this paper, we aim to clearly distinguish the geographic locations across the whole of Global South where addition of Phase Change Materials (PCM) would prove advantageous from the ones where it would be detrimental to the PV system efficiency. For the purpose of this communication, the term Global South refers broadly *to the regions of Latin America, Asia, Africa, and Oceania; "Third World" and "Periphery," that denote regions outside Europe and North America, mostly (though not all) low-income and often politically or culturally marginalized* (Dados & Connell, 2012).

In this study, the effectiveness of PCMs as a means to reduce the operating temperature of Concentrated Photovoltaic (CPV) panels in the Global South has been explored. Utilising lab-based experimental results from a CPV-PCM system, and a co-simulation approach using the software BCVTB, MATLAB and EnergyPlus, the panel surface temperature and CPV efficiency were simulated.

The results and conclusions from this study on one hand will help increase the understanding about the effectiveness of CPV-PCM systems as a whole and on the other hand assist decision makers with quantitative data for wide geographies to make appropriate investment decisions.

Literature review

PV performance in hot climates

The electrical efficiency of a PV panel has a linear correlation with the operating temperature; the PV material being a primary influence for the temperature sensitivity. For instance, the most commonly used crystalline silicon-based PV panels have a permissible degradation rate of 0.8 % per year with warranties for up to 25 years. The rates, however, demonstrate an annual median value of 0.5% as per an international review of the available field test results (Gaglia et al., 2017).

The key methods for PV cooling could be broadly classified into active and passive means depending on whether electrical power is used or not (through a pump, blower, or a fan). While forced air and water cooling fall under the category of active cooling, passive cooling includes natural/free convection of air and water, heat pipes, and use of PCM.

PV-PCM performance experimentation

Several authors from literature advocate PCM as an effective passive method for PV cooling for temperature reduction, increase in electrical output thereby positive environmental implications through reducing the use of energy-intensive silicon material. The effectiveness is determined by thermo-physical properties of the material as well as befitting external conditions such as irradiance, ambient temperature affecting the convection effect within the melted PCM, the wind velocity, and the angle of inclination of the PV panel as tilt angles and wind velocities are associated with lowering the operating temperatures (Kant et al., 2016).

In a study (Nada & El-Nagar, 2018), four different PV modules, namely, (a) a free-standing, (b) a building-integrated, (c) a PCM-integrated, and (d) a nano-enhanced PCM-integrated system were compared experimentally for temperatures distributions and output electrical parameters at a site in Egypt. The results showed that using PCM and nano-PCM increased the average daily power in free-standing PVs by 4.1% and 5.6% respectively. The peak power increase was 6.7% and 8.5% respectively. The building integrated PV showed high temperature rise (from 50 °C to 75 °C) compared to the free-standing and that the PCM addition was only effective for the free-standing PVs with a daily average efficiency increase by 7.1% (Nada & El-Nagar, 2018).

The efficiency of a vertical building-added PV-PCM system showed an average increase of 1.5% in the power output, while the peak increased by a maximum of 3% experimentally with the annual weather conditions taken into account (Park et al., 2014).

In a separate application, it was revealed that adding flat plate solar collectors, absorption chiller with fan coil, and PCM to the walls of a building could reduce the energy consumption by 450 kWh (Amirahmad et al., 2021).

The enviro-economic analysis on the impacts of various PV-cooling techniques on CO_2 emissions revealed that passive technologies such as nano-PCM, hybrid PCM, and hybrid PCM-water, respectively proved more effective than the use of individual techniques (Ghadikolaei, 2021).

PV-PCM performance modelling and simulation

A building integrated PV-PCM system installed on the building façade of an office was theoretically simulated and field-tested for the winter season in Lisbon, Portugal (Aelenei et al., 2014). The test prototype (0.73 m × 1.75 m) consisted of a polycrystalline PV-panel and a gypsum wallboard incorporating PCM Alba® balance type. A 1-D dynamic simulation program and a control-volume based finite-difference scheme was used through MATLAB/SIMULINK® with SIMSCAPE® library on a staggered grid. It was found that the thermal efficiency of the PV-PCM reached as high as 10% and an overall (thermal plus electrical) efficiency of about 20% with PCM (Aelenei et al., 2014). Unfortunately, a comparison with the baseline (no PCM) case was not provided in the study.

Integration of PCM with PV in glazed buildings was numerically studied using a 1-dimensional transient model using MATLAB/TRNSYS and validated with the experimental results (Elarga et al., 2017). The temperature profile of PCM on a buildings window, and with a PV layer was analysed. The overall numerical model was implemented to a double skin façade building with a PV-PCM layer in a ventilated cavity in Venice and Helsinki. It was revealed that a PV-PCM layer was sufficient to reduce the demand for cooling by 60% in Venice, and the demand for heating in Helsinki by 36% (Elarga et al., 2017). The authors noted that substantial amounts of heating/cooling energy demands could be met through building-integration of PV-PCM in Nordic countries, depending on the thermo-physical material properties.

A simulation study for PV-PCM system with the climatic conditions of Incheon, South Korea, demonstrated that the best outputs in terms of generated power were observed for October with high irradiance and moderate ambient temperature; later being an important criterion for PCM effectiveness (Park et al., 2014). Irrespective of the direction of installation, the PCM melting temperature of 298 K (~25°C) was found optimum.

In another simulation, the dynamic thermal performance model for a ventilated PV-PCM façade showed a peak shift time of over five hours, with a temperature reduction of over 20 °C (Curpek & Hraska, 2017). Design Builder software was used to study the climatic conditions of Bratislava (Slovakia) in this case.

Through the above literature review, it was identified that so far only a few studies have targeted the simulation of PV systems with PCM and within these, almost all of them focussed on one, two or a few global locations to test the effectiveness of PV-PCM systems. Therefore, we attempt to cover a majority of regions from the Global South to address this knowledge gap.

While the studies described in this section show that PCM-PV modelling has been carried out, the following research gaps were observed

- Generally, studies consider limited geographical locations, with very few studies done for Global South locations.
- Most studies employ simulation approaches that may not be easily integrated into Buildings Energy Modelling (BEM). Few studies use widely accepted BEM tools, such as DesignBuilder, but none analysed PCM integration into PV panels.

To address these gaps, this paper used an approach well suited for BEM and considers 885 locations in the Global South for assessing the PV-PCM potential. Moreover, the experimental data used for this study is for a CPV-PCM system fully tested in the laboratory with the concentrating element added to the study, which adds to the novelty of this research.

Methods

This study employs a co-simulation approach using BCVTB (Wetter et al., 2008) to couple MATLAB 2018b (Mathworks, 2021) and EnergyPlus v8.8 (EnergyPlus, 2012). Such an approch allows for modelling that is not readily available in EnergyPlus (Khattak et al., 2020). As a PCM integrated PV model was not available in EnergyPlus, this co-simulation approach was considered appropriate for this study. Laboratory experimental data is utilized within the simulation timestep while making use of the full simulation capability of EnergyPlus. While building performance is not analysed in this study, a typical mid-rise appartment reference building (DOE, 2020) was used where the PV were positioned horizontally on the roof. The co-simulation approach allowed us to understand how the efficiency of typical solar PV panels may be affected if PCM are integrated into them, while taking into account weather conditions for typical reference years across selected Global South locations. Moreover, the approach is suitable for Buildings Energy Modleling and can be utlised for another other experimental data set. The methodology employed is comprised of (i) selecting appropriate weather location where PCM can be fully charged and discharged and where the summers may be hot enough to necessitate PV surface temperature management (ii) experiment details for with and without PCM integrated into PVs (iii) co-simulation workflow. These are described as follows.

Geographical locations and weather data selection

The simulation methodology in this study employs EnergyPlus as the core simulation engine, for which weather data is in the form of hourly typical reference years, in EPW(Energy Plus Weather) format. In this study, all freely available epw files (3034 in total) were downloaded in bulk from (EnergyPlus, 2022). From the global dataset, there were 885 Global South location weather files which were then further analysed for PV-PCM suitability.

For PV-PCM systems to work effectively, it is imperative that the PCM undergo congealing or solidification during the non-sunny hours (Lazaro et al., 2009). For varying solar irradiance, ambient temperatures and other climatic parameters, the selection of an appropriate PCM material is indeed of paramount importance. Together with the fact that PV cooling is only required for locations where the elevated PV surface temperture may lead to lower efficiency, the 885 GS locations were further filtered into 128 locations across 17 countries using the following two criteria:

- A minimum of 10°C monthly average diurnal swing.
- A minimum peak summer temperature of 25°C.

It should be noted here that with such a climate selection, it is assumed that the PCMs completely charge and discharge over the passage of a day. This assumes careful selection of the PCM melting point with reference to the ambient temperature (Lazaro et al., 2009).

Experimental data

The indoor experimental work was carried out under the AAA Wacom Super Solar Simulator® (WXS-300S-50 AM1.5G) in the UK (Sharma et al., 2016). A CPV-PCM system was designed and fabricated in the laboratory. The key components for the experimental set up were:

i. A PV module with crystalline silicon solar cells (dimensions 116×6 mm^2) soldered in series using thin tin-plated copper strips, and assembled on a 0.6 mm thick Aluminium back plate.

ii. Optical elements or concentrators: linear asymmetric compound parabolic concentrator (LACPC) with acceptance half-angles as 0° and 55° providing a low geometrical concentration of ~2.7.

iii. PCM containment made using 13 mm thick Perspex sheet walls with the inner dimensions of 144×134×38 mm3.

iv. PCM Rubitherm RT-42® was used; latent heat capacity of 174 kJ/kg, and melting temperature range between 38-43°C.

v. The electrical connections and peripheral devices for measurements.

The CPV-PCM system was characterised performed using a highly collimated illumination from the solar simulator at 0° from horizontal.

The processes involved in manufacturing and assembling the system and further details on the thermo-physical properties of the components can be found from published literature (Sharma et al., 2016). The results showed an efficiency improvement in the CPV panel with the use of PCM at all the tested irradiance (500, 750, 1000 and 1200 Wm^{-2}) levels (Figure 1). The relative electrical efficiency improvements were 1.15%, 7.7%, 4.20% and at 6.80% at 500, 750, 1000 and 1200 Wm^{-2} respectively using PCM for passive cooling. A reduction in average temperature was noticed (6.2°C) in the centre of the CPV panel integrated with PCM compared to the naturally ventilated system.

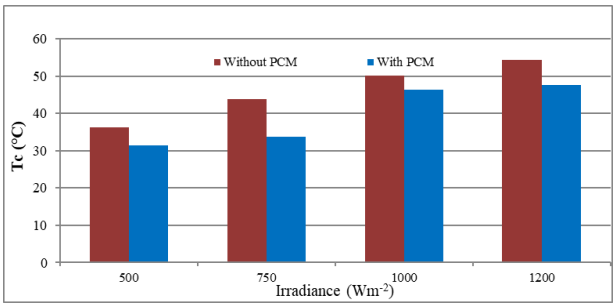

Figure 1: Temperature at the centre of the module without and with PCM at various irradiance levels. The average temperature reduction for the complete dataset is 6.2 °C

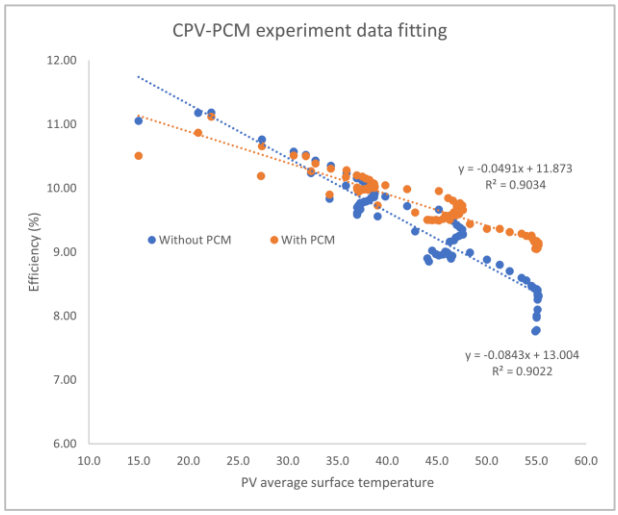

Figure 2: Effect of PCM on PV efficiency based on indoor lab experiments. Note that at a surface temperature greater than 33.3C, usage of PCM results in higher efficiency.

The PV average surface temperaure was plotted against the efficiency (Figure 2). A linear fit resulted in a R-squared value of 0.9034 and 0.9022 for PV with and without PCM respectively, to be used in the co-simulation setup.

Simulation workflow:

In this study, 128 locations had to be considered for two cases, with and without PCMs – within a co-simulation setup. While the co-simulation was managed by BCVTB, it was launched from MATLAB sequentially for the 128 location, updating the BCVTB xml file with the appropriate weather file before each simulation. This way, an autmated co-simiulation workflow was created, which in future studies could be easily expanded to consider different weather locations, building types and experimental data.

For each timestep (10min), EnergyPlus calculates the heat transfer for the interaction between the PV surface and the weather conditions. The simulated PV surface temperature dictates the PV efficiency which is read in MATLAB based on the linear relationships between PV surface temparature and efficiency from labwork (Figure 2). Thus, with this scheme, the heat transfer model of EnergyPlus is coupled with the lab data that qauntifies the effect of PCM on PV efficiency, whilst taking into account weather conditions for the typical reference year. It sould be noted from Figure 2 that PV efficiency only improves when the PV surface temperature is above 33.3°C. This is important because for any timepoint where the surface temperaure is below this, PCM will actually reduce PV efficiency. Thus, simulating for the fluctuating weather conditions over a year would help answer if PCMs could improve PV efficiency.

A limitation of this study is that indoor laboratory data was only available for a limited temperature range (15 < T < 55.2). An analysis of the 128 Global South weather files revealed that less than 1% of the total hours lie above 55.2°C but a substantial amount (40%) of data is at a PV surface temperature below 15°C. Therefore, the results of the colder climates within the global south for this study may underestimate the reduction in PV efficiency from PCM integration for such climates.

Results and Discussion:

Based on the hourly simulations for the typical year, Figure 3 shows the boxplots for each location for the baseline no-PCM case. For this particular CPV used in the laboratory, the average PV efficiency across the 128 locations ranged between 9-11% approximately. This data was based on efficiency for daylight hours only, as this is when the PV will actually operate. The actual locations corresponding to their serial numbers in Figure 3 and the remaining paper is provided in the Appendix.

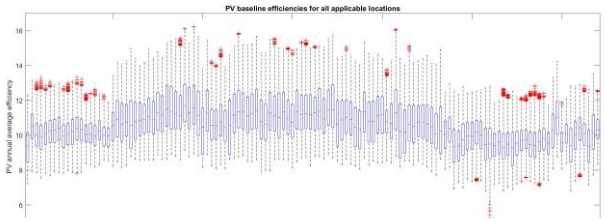

Figure 3: No-PCM PV baseline case annual efficiency boxplots for 128 GS locations

In order to assess the impact of integrating PCMs into PVs, the difference in average annual efficiencies between with and without PCM cases was calculated for the 128 locations. This absolute difference in average efficiencies was then plotted as a scatter chart, and the data colour coded using the baseline PV surface average annual temperature (Figure 4). The figure highlights the fact that the usefulness of PCM does indeed improve as the PV average surface temperature (and by association the climate) gets hotter.

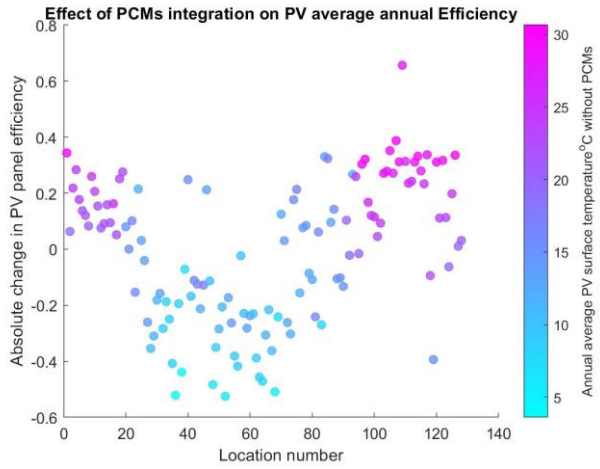

Figure 4: Effect of PCM on efficiency for the selected 128 Global south climates.

In the colder locations, especially when the average annual PV surface is below 15°C, PCMs result in PV efficiency reduction, up to 0.53% in location #52 (Dong Ujimqin Qi, China,. This was a reduction from 11.41% to 10.88%. On the other hand, for a hotter (location #109 ,Hissar, India), the absolute annual average PV efficiency increased by 0.66% (from 9.26% to 9.92%). This is a relative increase in efficiency of 7.13% over the naturally cooled PVs. However, from Figure 4, we observe that most locations had a lower absolute improvement in the range of 0.2% - 0.4%.

To better understand the results, the best and worst performing locations have been analysed in greater detail in Figures 5 and 6. The daytime profile (Figure 5(b)) shows that the amplitude of the PCM based PV is smaller for a period in April. This is also evident from the yearly data (Figure 5(a)) where PCM integration results in a more compressed histogram as compared to the no-PCM case. Qualitatively, one may say that integration of PCMs result in more consistent efficiency performance of PV by preventing the efficiency from excessively dropping during hot summer afternoons. Note that this is the timeframe when the maximum amount of solar radiation will be incident on the PV. In comparison, the worst performing location (#52) results in consistently worse off performance when PCMs are present (Figure 6). Here, the PV surface temperature stays below 33.3°C, where PCM results in lower efficiency. This is evident from the yearly histogram as well as daily PV surface profile during April in Figures 6(a) and 6(b).

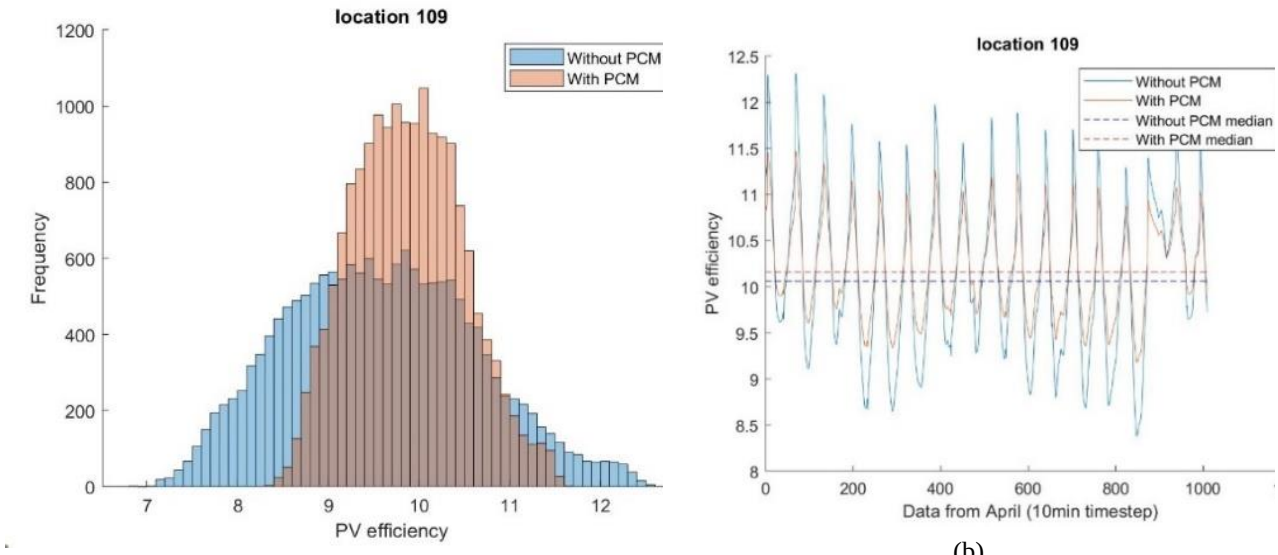

(a) (b)

Figure 5: Example location where PCM integration into PV is an advantage. Figure (a) is a yearly histogram showing that PCM integration results in an overall higher average efficiency. Figure (b) shows how the efficiency does not drop as low when PCM are present.

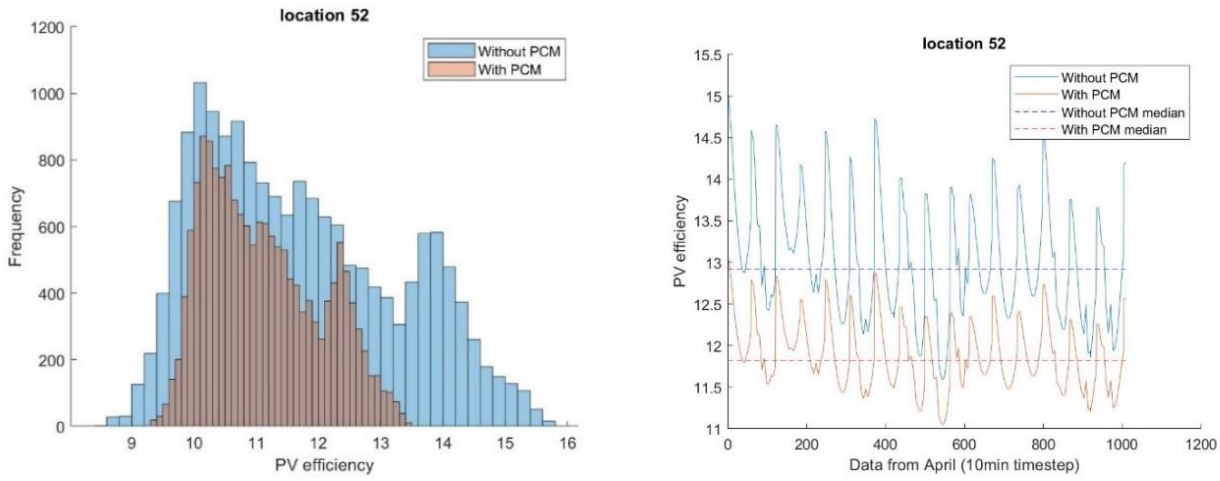

(a) (b)

Figure 6: Example location where PCM integration into PV is a disadvantage. Figure (b) shows the daytime profile in April when PCM lead to significantly lower efficiency, also evident from the yearly results (Figure (a)).

Conclusion

Based on the 885 Global South locations considered, 128 were identified with warm/hot summers where PCM could sufficiently charge and discharge over the daily cycle. Among these 128 locations, integration of PCMs into PVs resulted in a relative improvement of approximately 2% - 7% in average annual efficiency over naturally cooled PV in 36 locations. Here, the PCM reduced the amplitude of oscillations in PV efficiency over the daily cycle by reducing the daily maximum and minimum efficiencies achieved, resulting in a more consistent performance as compared to the non-PCM case. For the remaining locations, integration of PCM resulted in overall reduced performance, owing to an average elevated PV average surface temperature.

While the methodology presented in this study is an automated co-simulation approach which can utilize any other experimental data on PV performance, and it can be used for buildings energy modelling, it is cumbersome and slow to simulate. An improvement would be to couple the EnergyPlus PCM model into its PV model, which would remove the requirement for co-simulation. Nonetheless, the results of this study can be used to decide if such an effort is warranted.

References

Aelenei, L., Pereira, R., Gonçalves, H., & Athienitis, A. (2014). Thermal performance of a hybrid BIPV-PCM: modeling, design and experimental investigation. *Energy Procedia*, *48*, 474–483.

Amirahmad, A., Maglad, A. M., Mustafa, J., & Cheraghian, G. (2021). Loading PCM into buildings envelope to decrease heat gain-performing transient thermal analysis on nanofluid filled solar system. *Energy Res*, *9*, 727011.

Curpek, J., & Hraska, J. (2017). Simulation study on thermal performance of a ventilated PV façade coupled with PCM. *Applied Mechanics and Materials*, *861*, 167–174.

Dados, N., & Connell, R. (2012). The global south. *Contexts*, *11*(1), 12–13.

DOE. (2020). *Commercial reference buildings*. https://www.energy.gov/eere/buildings/commercial-reference-buildings

Elarga, H., Fantucci, S., Serra, V., Zecchin, R., & Benini, E. (2017). Experimental and numerical analyses on thermal performance of different typologies of PCMs integrated in the roof space. *Energy and Buildings*, *150*, 546–557. https://doi.org/10.1016/j.enbuild.2017.06.038

EnergyPlus. (2012). *Energy Simulation Software Version 8.1 [Online]*. US department of energy. http://apps1.eere.energy.gov/buildings/energyplus/ [Accessed: 6 December 2013]

EnergyPlus. (2022). *Weather Data*. https://energyplus.net/weather-region/europe_wmo_region_6

Gaglia, A. G., Lykoudis, S., Argiriou, A. A., Balaras, C. A., & Dialynas, E. (2017). Energy efficiency of PV panels under real outdoor conditions–An experimental assessment in Athens, Greece. *Renewable Energy*, *101*, 236–243.

Ghadikolaei, S. S. C. (2021). An enviroeconomic review of the solar PV cells cooling technology effect on the CO2 emission reduction. *Solar Energy*, *216*, 468–492.

Kant, K., Shukla, A., Sharma, A., & Biwole, P. H. (2016). Heat transfer studies of photovoltaic panel coupled with phase change material. *Solar Energy*, *140*, 151–161.

Khattak, S. H., Natarajan, S., & Chung, W. J. (2020). Out with the power outages : Peak load reduction in the developing world. *Windsor 2020 Resilient Comfort*, 904–922. https://core.ac.uk/download/pdf/323491371.pdf

Lazaro, A., Dolado, P., Marín, J. M., & Zalba, B. (2009). PCM–air heat exchangers for free-cooling

applications in buildings: Experimental results of two real-scale prototypes. *Energy Conversion and Management*, *50*(3), 439–443.

Mathworks. (2021). *MATLAB*. https://uk.mathworks.com/products/matlab.html

Nada, S. A., & El-Nagar, D. H. (2018). Possibility of using PCMs in temperature control and performance enhancements of free stand and building integrated PV modules. *Renewable Energy*, *127*, 630–641.

Park, J., Kim, T., & Leigh, S.-B. (2014). Application of a phase-change material to improve the electrical performance of vertical-building-added photovoltaics considering the annual weather conditions. *Solar Energy*, *105*, 561–574.

Sharma, S., Tahir, A., Reddy, K. S., & Mallick, T. K. (2016). Performance enhancement of a Building-Integrated Concentrating Photovoltaic system using phase change material. *Solar Energy Materials and Solar Cells*, *149*, 29–39. https://doi.org/https://doi.org/10.1016/j.solmat.2015.12.035

Wetter, M., Haves, P., & Coffey, B. (2008). *Building controls virtual test bed*. Lawrence Berkeley National Lab.(LBNL), Berkeley, CA (United States).

Appendix

Table 1: Location and EPW file names considered in this study

Location #	Location and EPW name	Location #	Location and EPW name
1	ARE_Abu.Dhabi.412170_IWEC.epw	40	CHN_Henan.Lushi.570670_CSWD.epw
2	ARG_Buenos.Aires.875760_IWEC.epw	41	CHN_Jilin.Linjiang.543740_CSWD.epw
3	ARG_Chaco_Resistencia.Intl.AP_871550_ArgTMY.epw	42	CHN_Kinjiang.Uygar.Kashi.517090_SWERA.epw
4	ARG_Chaco_Saenz.Pena.AP_871490_ArgTMY.epw	43	CHN_Kinjiang.Uygur.Kuqa.516440_SWERA.epw
5	ARG_Corrientes_Corrientes.Intl.AP_871660_ArgTMY.epw	44	CHN_Kinjiang.Uygur.Yining.514310_SWERA.epw
6	ARG_Corrientes_Paso.de.los.Libres.Intl.AP_872890_ArgTMY.epw	45	CHN_Kinjiang.Uyhur.Hotan.518280_SWERA.epw
7	ARG_Entre.Rios_Concordia_873950_ArgTMY.epw	46	CHN_Liaoning.Chaoyang.543240_CSWD.epw
8	ARG_Entre.Rios_Gualeguaychu.AP_874970_ArgTMY.epw	47	CHN_Liaoning.Kuandian.544930_CSWD.epw
9	ARG_Formosa_Formosa.Intl.AP_871620_ArgTMY.epw	48	CHN_Nei.Mongol.Abag.Qi.Hot.531920_CSWD.epw
10	ARG_Misiones_Puerto.Iguazu.Intl.AP_870970_ArgTMY.epw	49	CHN_Nei.Mongol.Bairin.Zuo.Qi.540270_CSWD.epw
11	ARG_Santa.Fe_Ceres_872570_ArgTMY.epw	50	CHN_Nei.Mongol.Bayan.Mod.524950_CSWD.epw
12	ARG_Santa.Fe_Rosario.Intl.AP_874800_ArgTMY.epw	51	CHN_Nei.Mongol.Chifeng.542180_CSWD.epw
13	ARG_Santa.Fe_Sauce.Viejo.AP_873710_ArgTMY.epw	52	CHN_Nei.Mongol.Dong.Ujimqin.Qi.509150_CSWD.epw
14	BRA_Brasilia.833780_IWEC.epw	53	CHN_Nei.Mongol.Ejin.Qi.522670_CSWD.epw
15	BRA_Brasilia.833780_SWERA.epw	54	CHN_Nei.Mongol.Ejin.Qi.522670_SWERA.epw
16	BRA_Campo.Grande.836120_SWERA.epw	55	CHN_Nei.Mongol.Erenhot.530680_CSWD.epw
17	BRA_DF_Brasilia-Kubitschek.Intl.AP.833780_TRY.1962.epw	56	CHN_Nei.Mongol.Hailisu.532310_CSWD.epw
18	BRA_PR_Londrina.837680_INMET.epw	57	CHN_Nei.Mongol.Haliut.533360_CSWD.epw
19	BRA_SP_Campinas.837210_INMET.epw	58	CHN_Nei.Mongol.Hohhot.534630_CSWD.epw
20	CHL_Santiago.855740_IWEC.epw	59	CHN_Nei.Mongol.Jartai.535020_CSWD.epw
21	CHN_Beijing.Beijing.545110_CSWD.epw	60	CHN_Nei.Mongol.Jartai.535020_SWERA.epw
22	CHN_Beijing.Beijing.545110_IWEC.epw	61	CHN_Nei.Mongol.Jarud.Qi.540260_CSWD.epw
23	CHN_Beijing.Beijing.545110_SWERA.epw	62	CHN_Nei.Mongol.Jurh.532760_CSWD.epw
24	CHN_Gansu.Jiuquan.525330_CSWD.epw	63	CHN_Nei.Mongol.Linxi.541150_CSWD.epw
25	CHN_Gansu.Lanzhou.528890_CSWD.epw	64	CHN_Nei.Mongol.Linxi.541150_SWERA.epw
26	CHN_Gansu.Lanzhou.528890_IWEC.epw	65	CHN_Nei.Mongol.Otog.Qi.535290_CSWD.epw
27	CHN_Gansu.Lanzhou.528890_SWERA.epw	66	CHN_Nei.Mongol.Tongliao.541350_CSWD.epw
28	CHN_Gansu.Yumenzhen.524360_CSWD.epw	67	CHN_Nei.Mongol.Tongliao.541350_SWERA.epw
29	CHN_Gansu.Yumenzhen.524360_SWERA.epw	68	CHN_Nei.Mongol.Xi.Ujimqin.Qi.540120_CSWD.epw
30	CHN_Hebei.Fengning.543080_CSWD.epw	69	CHN_Nei.Mongol.Xilinhot.541020_CSWD.epw
31	CHN_Hebei.Huailai.544050_CSWD.epw	70	CHN_Ningxia.Hui.Yinchuan.536140_CSWD.epw
32	CHN_Heilongjiang.Anda.508540_CSWD.epw	71	CHN_Shaanxi.Yanan.538450_CSWD.epw
33	CHN_Heilongjiang.Harbin.509530_CSWD.epw	72	CHN_Shaanxi.Yulin.536460_CSWD.epw
34	CHN_Heilongjiang.Harbin.509530_IWEC.epw	73	CHN_Shaanxi.Yulin.536460_SWERA.epw
35	CHN_Heilongjiang.Harbin.509530_SWERA.epw	74	CHN_Shandong.Weifang.548430_CSWD.epw
36	CHN_Heilongjiang.Huma.503530_CSWD.epw	75	CHN_Shandong.Yanzhou.549160_CSWD.epw
37	CHN_Heilongjiang.Mudanjiang.540940_CSWD.epw	76	CHN_Shanxi.Datong.534870_CSWD.epw
38	CHN_Heilongjiang.Nenjiang.505570_CSWD.epw	77	CHN_Shanxi.Jiexiu.538630_CSWD.epw
39	CHN_Heilongjiang.Tonghe.509630_CSWD.epw	78	CHN_Shanxi.Taiyuan.537720_CSWD.epw

Table 1: Location and EPW file names considered in this study

79	CHN_Shanxi.Yuanping.536730_CSWD.epw
80	CHN_Shanxi.Yushe.537870_CSWD.epw
81	CHN_Sichuan.Batang.562470_SWERA.epw
82	CHN_Xinjiang.Uygur.Bachu.517160_CSWD.epw
83	CHN_Xinjiang.Uygur.Fuyun.510870_CSWD.epw
84	CHN_Xinjiang.Uygur.Hami.522030_CSWD.epw
85	CHN_Xinjiang.Uygur.Hotan.518280_CSWD.epw
86	CHN_Xinjiang.Uygur.Jinghe.513340_CSWD.epw
87	CHN_Xinjiang.Uygur.Kashi.517090_CSWD.epw
88	CHN_Xinjiang.Uygur.Kuqa.516440_CSWD.epw
89	CHN_Xinjiang.Uygur.Minfeng.518390_CSWD.epw
90	CHN_Xinjiang.Uygur.Tikanlik.517650_CSWD.epw
91	CHN_Xinjiang.Uygur.Turpan.515730_CSWD.epw
92	CHN_Xinjiang.Uygur.Turpan.515730_SWERA.epw
93	CHN_Xinjiang.Uygur.Yining.514310_CSWD.epw
94	CHN_Yunnan.Mengla.569690_CSWD.epw
95	DZA_Algiers.603900_IWEC.epw
96	EGY_Aswan.624140_ETMY.epw
97	EGY_Aswan.624140_IWEC.epw
98	EGY_Asyut.623930_ETMY.epw
99	EGY_Cairo.623660_IWEC.epw
100	EGY_Cairo.Intl.Airport.623660_ETMY.epw
101	EGY_El.Arish.623370_ETMY.epw
102	EGY_Ismailia.624400_ETMY.epw
103	EGY_Kharga.624350_ETMY.epw
104	EGY_Luxor.624050_ETMY.epw
105	IND_Akola.429340_ISHRAE.epw
106	IND_Bhopal.426670_ISHRAE.epw
107	IND_Bikaner.421650_ISHRAE.epw
108	IND_Gwalior.423610_ISHRAE.epw
109	IND_Hissar.421310_ISHRAE.epw
110	IND_Indore.427540_ISHRAE.epw
111	IND_Jabalpur.426750_ISHRAE.epw
112	IND_Jagdelpur.430410_ISHRAE.epw
113	IND_Jaipur.423480_ISHRAE.epw
114	IND_Jodhpur.423390_ISHRAE.epw
115	IND_Lucknow.423690_ISHRAE.epw
116	IND_Pune.430630_ISHRAE.epw
117	IND_Sholapur.431170_ISHRAE.epw
118	IRN_Shiraz.408480_ITMY.epw
119	IRN_Tabriz.407060_ITMY.epw
120	KEN_Garissa.637230_SWERA.epw
121	KEN_Makindu.637660_SWERA.epw
122	KWT_Kuwait.Intl.AP.405820_KISR.epw
123	LBY_Tripoli.620100_IWEC.epw
124	MAR_Casablanca.Nouasser.601560_IWEC.epw
125	PRY_Asuncion.862180_IWEC.epw
126	SAU_Riyadh.404380_IWEC.epw
127	SYR_Damascus.400800_IWEC.epw
128	ZWE_Harare.677750_IWEC.epw